

Article

Numerical Investigation of a Reactivity-Controlled Compression Ignition Engine Fueled with N-Heptane and Iso-Octane

Serdar Halis ^{1,*}, Hamit Solmaz ², Seyfi Polat ³ and H. Serdar Yücesu ²¹ Department of Automotive Engineering, Faculty of Technology, Pamukkale University, Denizli 20160, Turkey² Department of Automotive Engineering, Faculty of Technology, Gazi University, Ankara 06500, Turkey; hsolmaz@gazi.edu.tr (H.S.); yucesu@gazi.edu.tr (H.S.Y.)³ Department of Mechanical Engineering, Faculty of Engineering, Hitit University, Corum 19040, Turkey; seyfiolat@hitit.edu.tr

* Correspondence: shalis@pau.edu.tr

Abstract: In this numerical study, the effects of the premixed ratio, intake manifold pressure and intake air temperature on a four-cylinder, four-stroke, direct injection, low-compression-ratio gasoline engine, operated in reactivity-controlled compression ignition (RCCI) combustion mode at a constant engine speed of 1000 rpm, were investigated using Converge CFD software. The results of numerical analyses showed that the maximum in-cylinder pressure and heat release rate (HRR) increased and the combustion phase advanced depending on the rise in both intake manifold pressure and intake air temperature. The CA₅₀ shifted by 18.5 °CA with an increment in the intake air temperature from 60 °C to 100 °C. It was observed that the combustion duration dropped from 44 °CA to 38 °CA upon boosting the intake manifold pressure from 103 kPa to 140 kPa. Moreover, a delay in the combustion phase occurred at a constant intake air temperature with an increasing premixed ratio. The maximum value of in-cylinder pressure was recorded as 36.15 bar (at 11 °CA aTDC) with the use of PRF20. Additionally, as the content of iso-octane in the fuel mixture was increased, combustion delay occurred, and the maximum value of in-cylinder temperature obtained was 11 °CA aTDC using PRF20 fuel at the earliest point. While HC and CO emissions reached the highest values at a 60 °C intake air temperature, NO_x and soot emission values were detected at quite low levels at this temperature. The values of all these emissions increased with rising intake manifold pressure and reached their highest values at 140 kPa. In addition, while the highest HC and CO emission values were observed with the use of PRF60 fuel, the results revealed that the control of the combustion phase in the RCCI strategy is notably affected by the premixed ratio, intake manifold pressure and intake air temperature.

Keywords: RCCI; combustion; intake air temperature; intake manifold pressure; premixed fuel ratio; CFD; emission



Citation: Halis, S.; Solmaz, H.; Polat, S.; Yücesu, H.S. Numerical Investigation of a Reactivity-Controlled Compression Ignition Engine Fueled with N-Heptane and Iso-Octane. *Sustainability* **2023**, *15*, 10406. <https://doi.org/10.3390/su151310406>

Academic Editor: Ali Bahadori-Jahromi

Received: 11 June 2023

Revised: 22 June 2023

Accepted: 29 June 2023

Published: 1 July 2023



Copyright: © 2023 by the authors. Licensee MDPI, Basel, Switzerland. This article is an open access article distributed under the terms and conditions of the Creative Commons Attribution (CC BY) license (<https://creativecommons.org/licenses/by/4.0/>).

1. Introduction

Recently, there has been an increase in the cost of oil resources due to a reduction in the amount of them. Moreover, exhaust emissions have caused serious environmental pollution due to the increase in the use of vehicles. Scientists have focused on alternative combustion modes with high efficiency and low emissions in the face of these negative conditions [1–3]. Although spark ignition (SI) and compression ignition (CI) internal combustion engines have high power density and performance, in SI engines, a compression ratio (CR) higher than 14 cannot be applied due to the knock limit. In addition, SI engines are known to have low energy conversion efficiency at high loads and high CO emissions [4,5]. CI engines also have high soot emission, which may occur due to the heterogeneity of the mixture and high nitrogen oxide (NO_x) emission values due to high temperatures [6]. The use of after-treatment systems to prevent these emissions is mandatory and costly. These problems expose disadvantages in the use of SI and CI engines. Considering these negative

effects, a new combustion mode has been developed that represents low-temperature combustion technology, and involves a combination of the combustion processes of SI and CI engines [7,8].

Some low-temperature combustion modes include homogeneous charged compression ignition (HCCI), premixed charge compression ignition (PCCI) and reactivity-controlled compression ignition (RCCI) [9]. In HCCI engines, the air fuel mixture is taken into the cylinder as in spark ignition engines. Combustion takes place via simultaneous self-ignition of the homogeneous air–fuel mixture towards the end of the compression stroke. In this low-temperature combustion mode, thermal efficiency is also high due to the need for a high compression ratio [10–12]. Since HCCI engines can work with homogeneous lean mixtures, the in-cylinder gas temperatures at the end of combustion are lower than in SI and CI engines. Thanks to the low gas temperatures at the end of combustion, very low levels of NO_x are released [13,14]. The start of combustion (SOC) and the combustion rate are different in each cycle due to the fuel properties and auto-ignition. The severe knocking that occurs as a result of simultaneous homogeneous flash combustion, which increases the pressure rise rate and leads to high fluctuation in pressure, causes low thermal efficiency and cyclical variations. In addition, the operational range of an engine with HCCI combustion mode is very limited due to the increased knocking at high loads and the problem of misfire at low loads. The inability to control combustion, narrow operating range, high carbon monoxide (CO) and unburned hydrocarbon (UHC) emissions are seen as the biggest challenges in HCCI engines [15]. In HCCI engines, some methods, such as changing the octane number [16], increasing the intake air temperature [17], exhaust gas recirculation (EGR) [18] and the use of alternative fuels [19], different compression ratios [20,21], different intake manifold pressures [22–24] and different injection timings [25], are used to expand the operating range and to control the combustion process.

Researchers developed the RCCI combustion mode using two fuels of different reactivity in order to overcome the disadvantages of the HCCI combustion mode [26,27]. In the RCCI mode, a low-reactivity fuel LRF (e.g., gasoline, ethanol, methanol, etc.) is injected via port fuel injection, and a high-reactivity fuel HRF (e.g., diesel, dimethyl ether, etc.), which acts as the ignition source, is injected via direct injection [28,29]. The combustion phase can be controlled using a mixed ratio of LRFs and HRFs in the cylinder; thus, knocking can be decreased by controlling heat release, and NO_x and soot emissions can be significantly reduced. In addition, the combustion phase can be controlled by the injection timing of the fuels. Moreover, engines operating in RCCI mode have higher thermal efficiency than engines with conventional combustion modes thanks to controlled combustion [30,31]. A gasoline–air mixture cannot be ignited without diesel, as gasoline has poor auto-ignitability at low compression ratios. In their study forming the basis of the RCCI combustion mode, Kokjohn et al. [26] injected gasoline via port injection and diesel fuel via direct injection. The ratio of gasoline/diesel and injection timing can be used for controlling combustion. It was stated that 50% thermal efficiency and lower fuel consumption were achieved compared to diesel or gasoline engines. RCCI depends on the homogeneity of the mixture and the stratification of ignitability. This stratification can be easily controlled by spraying diesel fuel via direct injection. In RCCI mode, combustion progression from the high-reactivity region to the low-reactivity region significantly decreases the pressure rise rate (PRR) [32,33]. In a study conducted to examine how fuel properties affect RCCI combustion at low loads, both a dual fuel strategy and a single fuel strategy using gasoline with a 2-ethylhexylnitrate additive as an ignition improver were used. The indicated thermal efficiency (ITE) of 54% was achieved with the addition of additives, using gasoline as the single fuel [34]. Uyumaz and Solmaz [35] investigated the effect of injection timing on combustion characteristics in RCCI engines. It was observed that as the lambda diminished in a gasoline engine run at different lambda values, the heat release and maximum cylinder pressure increased. It was stated that the maximum ITE obtained was 42.47% at an injection timing of 80 °CA before top dead center (bTDC), with lambda value of 2.2. The study revealed that when the timing of direct injection was earlier than normal, the mixture was more homogeneous than

in HCCI combustion. In a study conducted to investigate the combustion characteristics and thermal efficiency of an RCCI engine for a wide range of engine speeds and loads, it was observed that there was a maximum 5% improvement in thermal efficiency and a 92% reduction in NO_x emissions compared to conventional diesel combustion [36]. Some parameters affecting RCCI combustion characteristics and emissions are also investigated numerically. Kakaee et al. [37] investigated the emissions and combustion characteristics of RCCI mode in a diesel engine using the KIVA–CHEMKIN code with gasoline and diesel used as fuel. It was stated that the PRR in RCCI combustion could be controlled by ratios of fuels and the timing of the start of injection (SOI) of diesel fuel. In a study investigating the effects of high-compression piston design to improve RCCI combustion and emissions, the authors reported that the indicated mean effective pressure (IMEP) achieved was 18 bar using gasoline–diesel in RCCI mode at an exhaust gas recirculation (EGR) of 35%. The direct injection of diesel fuel at different times was carried out for this analysis. The results showed that the changing of EGR affected RCCI combustion at high load [38]. In addition, since combustion temperature decreases with the dilution and thermal effects of EGR, a reduction in soot emissions and NO_x has been observed [39]. Hasankola et al. [40] numerically investigated intake valve closing temperature (T_{IVC}) and EGR's effects on an RCCI engine's emissions and performance, and the software CHEMKIN II and AVL FIRE were used in the numerical analyses. The natural gas was sprayed via port injection as an LRF, while the diesel fuel was directly sprayed into the cylinder as an HRF. The simulation results showed that as the EGR increased, the maximum pressure in the cylinder, the maximum heat release rate, and NO_x and soot emissions were reduced. In addition, an increase in the maximum pressure, HRR, and NO_x and soot emissions was observed due to the increase in the T_{IVC} .

In this study, a four-stroke four-cylinder gasoline engine was operated in RCCI mode at a 9.2:1 compression ratio, 80 °C intake air temperature and a constant engine speed of 1000 rpm. The influences of intake air temperature, intake manifold pressure and a pre-mixed ratio of fuels on combustion and emission characteristics in a low-compression-ratio gasoline engine operated in RCCI mode were investigated numerically, with the validation of experimental results, using Converge CFD computer software. Conventional combustion modes have low energy efficiency and damage the environment with their high emission levels. In particular, their inability to reduce soot and NO_x emissions simultaneously is a major problem. The RCCI combustion mode has a high energy conversion efficiency (up to 59% of the indicated thermal efficiency [27]), thereby contributing to sustainable energy utilization. In addition, the reduction in soot and NO_x emissions simultaneously will have a positive effect on the environment. This numerical study aims to contribute to the development of sustainable clean-energy technologies by using low-temperature combustion modes that promise high thermal efficiency and low emission levels.

2. Methodology

2.1. Experimental Setup

Experiments were conducted using iso-octane/n-heptane in a direct-injection, four-cylinder, four-stroke, 2.0 L, gasoline GM Ecotec engine operating in RCCI mode. The technical properties of the engine used in the experiments, carried out at Michigan Technological University (at the Research Center for Advanced Power Systems), are given in Table 1.

The test engine was connected to a 460 HP adjustable AC dynamometer; thus, the engine load and speed were controlled. An external fuel pump and electric motor were used for the fuel system. The intake air temperature was controlled by an air heater. The control of the air heater was carried out via dSPACE. An air filter mounted in front of a supercharger has a significant effect on the performance of the intake system and causes a certain pressure drop [41,42]. The air filter also has a considerable effect on the flow resistance [43,44].

Table 1. Detailed technical properties of test engine.

Engine Model	GM Ecotec GDI Turbo DOHC
Stroke × bore	86 mm × 86 mm
Cylinder number	4
Displacement	2.0 L
CR	9.2:1
Max. power	270 kW@6000 rpm
Max. torque	353 Nm@2400 rpm
IVC	−147 °CA aTDC
EVO	135 °CA aTDC

Eight low-pressure-port-type fuel (PFI) injectors were subsequently assembled on the engine's intake manifold. Four of these were used while the engine was operating in RCCI mode. Iso-octane as an LRF was sprayed using PFI injectors with 3 bar injection pressure, and n-heptane as an HRF was injected into the cylinder at 100 bar pressure via direct injection (DI). The features of the n-heptane and iso-octane fuels used in the experiments are shown in Table 2.

Table 2. Features of n-heptane and iso-octane [45,46].

Properties	N-Heptane	Iso-Octane
Formula	C ₇ H ₁₆	C ₈ H ₁₈
LHV (MJ/kg)	44.56	44.30
Molar mass (g/mol)	100.2	114.2
Density (kg/m ³)	686.6	693.8
Boiling point (°C)	371	372.4
Research octane number	0	100

A 115A04 model PCB piezotronics pressure transducer was used for in-cylinder pressure measurement in the combustion analysis. The measured in-cylinder pressure was amplified using a charge amplifier (DSP 1104CA) and processed using an ACAP analysis system. An encoder with a sensitivity of 1 °CA was connected to the engine. Fuel consumption was determined using a Coriolis-type fuel-flow meter (Micro Motion 1700).

Control of the RCCI motor was achieved using MicroAutoBox, dSPACE and RapidPro. Control of throttle body, high-pressure fuel pump, variable valve timing and injectors was achieved using the MATLAB Simulink model, which is embedded in the processor. Parameters influencing engine control, such as pressure of fuel rail, ignition system, position of cam, premixed ratio, position of throttle body, EGR valve position, pressure and intake air temperature, were controlled using dSPACE.

In Figure 1, a diagram of the test bed is displayed. The chassis system (NI PXIe-1078) was used for measurements of the thermocouple (NI TB-4353) and pressure transducer (NI PXI-6225), and for control of the dynamometer (NI PXI-6722). LabVIEW was used to display the obtained data. An emission analyzer was used for CO, CO₂, NO_x, HC and O₂ emission measurements in the experiments.

Specific fuel consumption (SFC), mean effective pressure (IMEP), maximum in-cylinder pressure and temperature, heat release rate (HRR), integrated heat release rate (IHRR), volumetric efficiency, maximum pressure rise rate (MPRR), thermal efficiency, combustion efficiency, CA50 and coefficient of variation of IMEP (COV_{IMEP}) were computed using a developed MATLAB code.

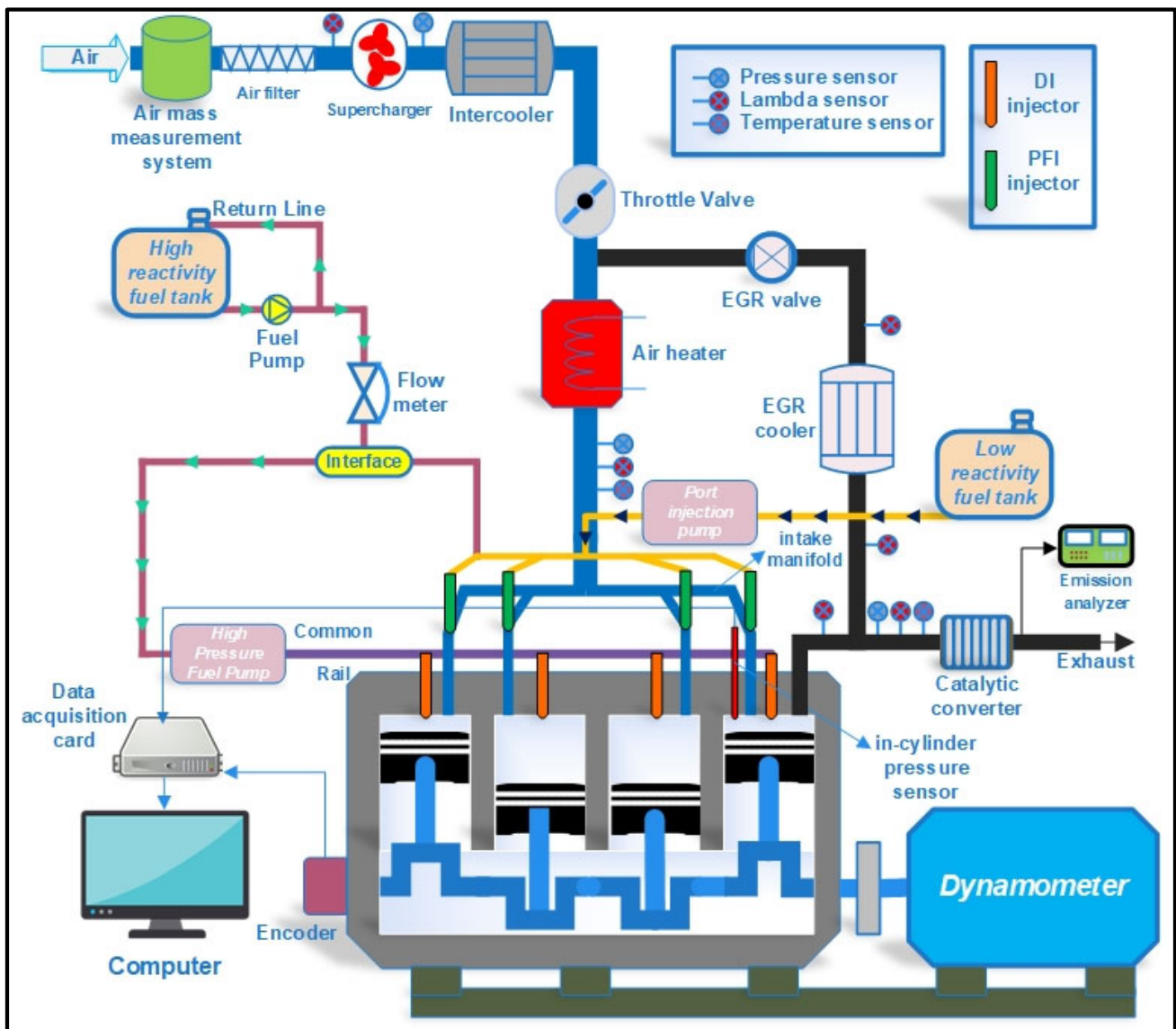


Figure 1. Diagram of the test bed.

The HRR was calculated using Equation (1) according to the first law of thermodynamics [47].

$$\frac{dQ}{d\theta} = \frac{k}{k-1} P \frac{dV}{d\theta} + \frac{1}{k-1} V \frac{dP}{d\theta} + \frac{dQ_{heat}}{d\theta} \quad (1)$$

where P , V , dQ , dQ_{heat} , $d\theta$ and k are in-cylinder pressure, cylinder volume, heat release, heat transfer to the cylinder walls, change in crank angle and ratio of specific heats, respectively.

2.2. Numerical Model

The CFD method was used with CONVERGE CFD software to simulate RCCI combustion. CONVERGE is a CFD program consisting of pre-process, process and post-process sections. CONVERGE automatically forms an excellently orthogonal, well-structured grid at run-time based on easy grid control variables. This method for the generation of grids at run-time completely overcomes the need for the manual generation of grids. The CONVERGE pre-processor CONVERGE Studio (Graphical User Interface) was used to form the case setup. Then, the compiled input files were run on the workstation, and the results were obtained via precision analysis [48].

The characteristics of the GM Ecotec GDI Turbo engine used in the simulations are given in Table 1. The geometry, including the total cylinder volume of the RCCI engine, was sketched using SOLIDWORKS software. Then, CONVERGE CFD was used for the meshing process, as this software provides auto-mesh refinement. Adaptive mesh refinement (AMR), which makes the mesh structure sensitive in the required regions, can be used in CONVERGE. The geometry of the model and the mesh process are seen in Figure 2. The mesh structure approximately consists of 550,867 cells.

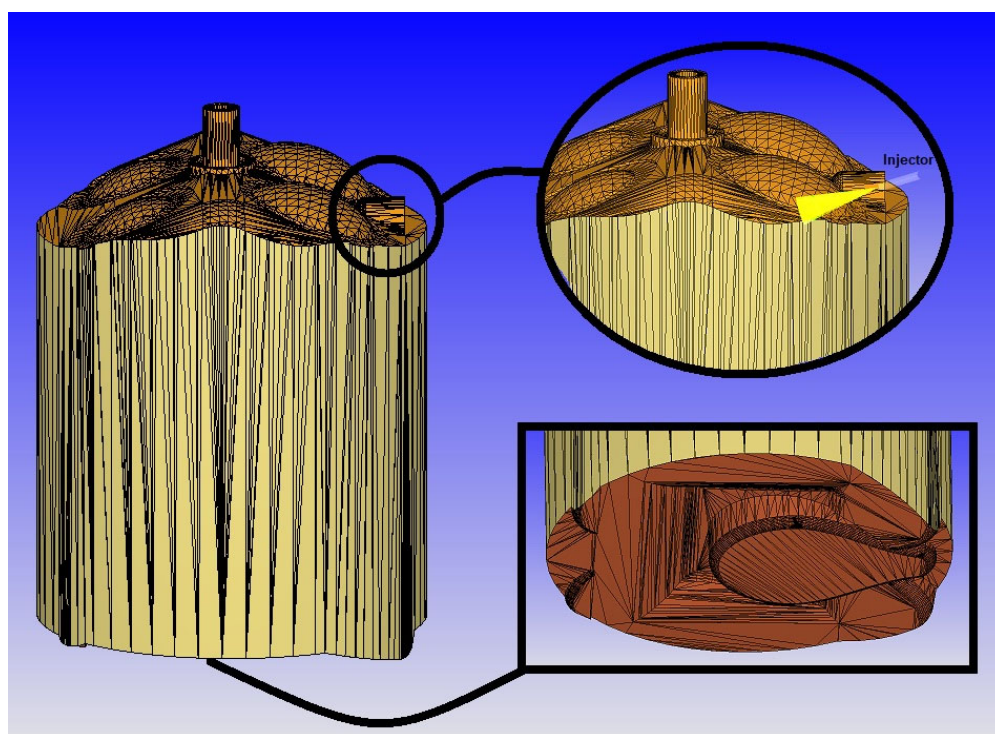


Figure 2. Demonstration of the geometry and mesh structure.

This numerical study was carried out as a closed cycle between IVC and EVO. Air and iso-octane injected via port injection were considered to be homogeneously mixed upon intake valve closing. The n-heptane direct injection procedure was simulated using the Discrete Droplet Model (DDM) [49]. The hybrid Kelvin–Helmholtz (KH)–Rayleigh–Taylor (RT) model, which consists of primary and secondary breakups, was used as a spray atomization model. KH and RT instabilities are responsible for the breakup length, while KH is responsible for drop breakup in the characteristic breakup distance [50]. The Renormalized Group (RNG) $k-\epsilon$ /Reynolds Averaged Navier–Stokes (RANS) was used to calculate turbulence in this numerical study [51]. In all the analyses, the values of the Prandtl and Schmidt numbers were assumed to be 0.9 and 0.78, respectively. The PISO method was used for solving discrete equations in CONVERGE. The velocity field was determined using momentum equations [52]. The SAGE detailed chemical kinetics solver was used for combustion modeling [53]. A PRF chemical kinetic mechanism including n-heptane and iso-octane, with 171 species and 861 reactions, was used in the numerical analyses. RCCI combustion was simulated using this mechanism, which was developed by Luang et al. [54].

The validation case setup of the RCCI engine is shown Table 3. It can be concluded that the validation process was successfully performed upon comparing the numerical results with the experimental results. The change in in-cylinder pressure and HRR depending on the crank angle obtained in the validation process is seen in Figure 3. According to results of the simulations, RCCI combustion with iso-octane and n-heptane was effectively analyzed by complying with the real experimental conditions. Therefore, the simulations

are thought to be reliable. It can be seen that the max. HRR from the experiments and max. HRR from the simulations are $79.29 \text{ J}/^\circ\text{CA}$ and $77.91 \text{ J}/^\circ\text{CA}$, respectively.

Table 3. Validation case setup of RCCI engine at initial stage.

Port Injection Fuel	Iso-Octane (20%)
Direct injection fuel	n-heptane (80%)
Engine speed	1000 rpm
Start of direct injection	-25°CA aTDC
Injection pressure	100 bar
Intake air temperature	80°C
Total fuel mass	22 mg/cycle
Intake manifold pressure	103 kPa
Lambda	1.2
Mesh size	1 mm
AMR level	3
Cylinder wall temperature	545 K
Minimum time step	$1 \times 10^{-8} \text{ s}$
Maximum time step	$1 \times 10^{-4} \text{ s}$

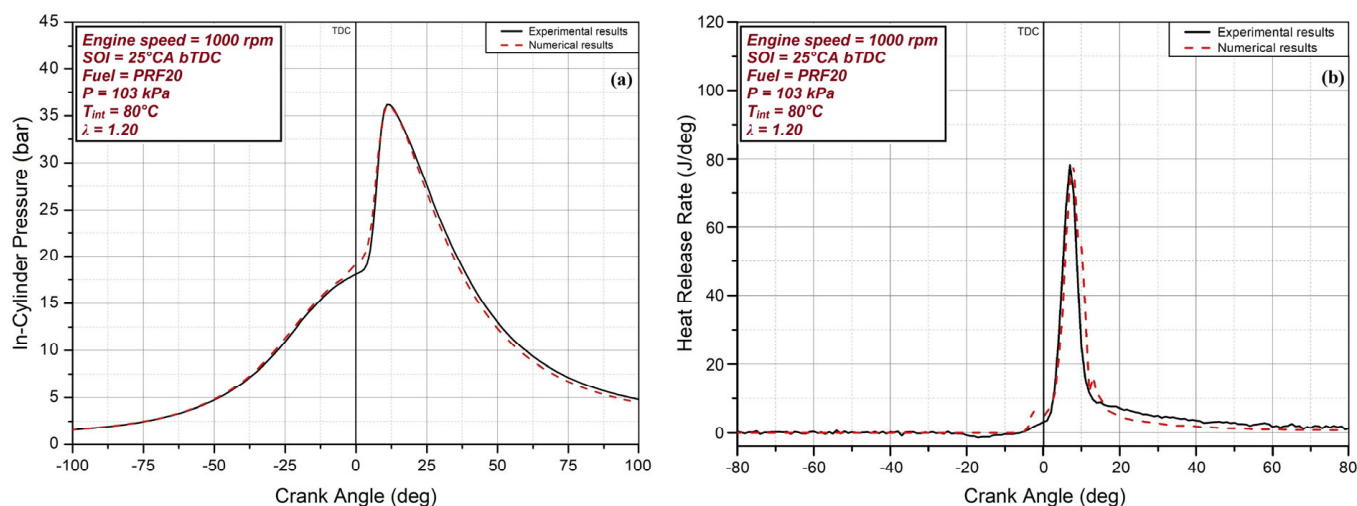


Figure 3. Validation of (a) in-cylinder pressure and (b) HRR.

3. Results and Discussion

The simulation results were validated based on the experiments carried out under the conditions mentioned above. An extensive simulation study was performed to investigate the effects of intake manifold pressure, premixed fuel ratio and intake air temperature on RCCI combustion.

3.1. Intake Air Temperature's Effects on RCCI Combustion

Figure 4 displays the change in the in-cylinder pressure and HRR at different intake air temperatures (60°C , 80°C and 100°C). RCCI combustion shows a lower heat release gradient and lower cylinder pressure than the other conventional combustion types. RCCI combustion has longer and slower heat release than conventional diesel combustion. These results are consistent with those in the study of Pohlkamp and Reitz [55].

The maximum cylinder pressure increases and the combustion is advanced as the intake air temperature increases. This situation influences the thermal efficiency and combustion. There is a significant increase in reactivity with increasing intake air temperature. The results show that combustion is significantly advanced and the maximum pressure increases, especially at an intake air temperature of 100°C . After a certain value, the volumetric efficiency is significantly reduced due to the low density of the intake air. The lower

volumetric efficiency causes the engine to operate at lower loads, which can bring about a delay at the start of combustion.

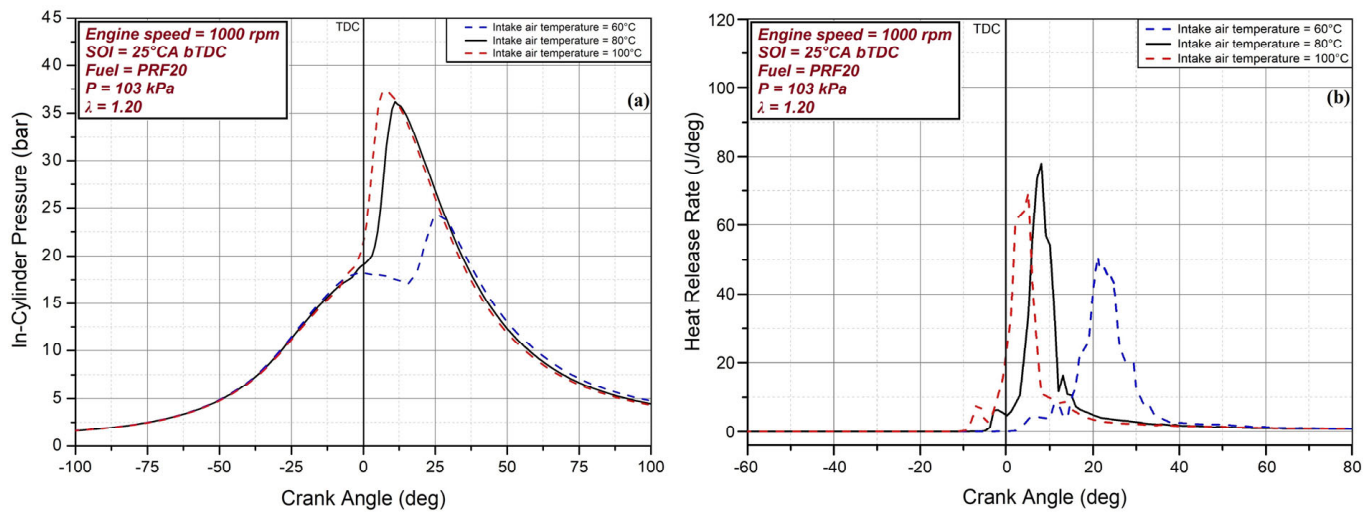


Figure 4. Change in (a) in-cylinder pressure and (b) HRR at various intake air temperatures.

RCCI combustion is a type of premixed combustion controlled by chemical kinetics. The high intake air temperature prevents the cylinder wall temperature from decreasing too much; thus, the combustion is improved. This is because the cold cylinder wall causes a decrease in the kinetic reaction rate and adversely affects the combustion in RCCI mode [56].

Combustion duration is equal to the difference between the crank angle of 90% (CA90) and the crank angle of 10% (CA10) of the total heat released. The crank angle corresponding to 50% of the total heat release is called CA50. CA50 and combustion duration (CA90-CA10) can affect the cyclic variability, controllability and tendency for knocking [57,58]. The CA50 is equal to 23 °CA, 8.5 °CA and 4.5 °CA aTDC for intake air temperatures of 60 °C, 80 °C and 100 °C, respectively.

The results show that higher values of intake air temperature increase CA50, and the combustion duration is also decreased noticeably. When intake air temperature goes up from 60 °C to 100 °C, the CA50 shifts by 18.5 °CA.

For low-temperature combustion strategies such as HCCI and RCCI, the charge air is heated and taken into the cylinder in order to achieve better combustion. Figure 5 presents the effects of intake air temperature on HC, CO, NO_x and soot emissions for RCCI combustion. The lower the intake air temperature, the lower the in-cylinder temperature tends to be, and incomplete combustion products are also produced. This is why it is seen that HC emissions are much higher at low temperatures. A similar situation is also observed for CO emissions. The maximum values of these emissions were recorded at a 60 °C intake air temperature. As the intake air temperature is increased, the temperature profile in the cylinder tends to drop less than the previous temperature value. Therefore, the increase in intake air temperature causes more NO_x to be released. Soot emission also reaches higher emission levels with increasing intake air temperature. However, the NO_x and soot emission values obtained in this numerically investigated low-temperature combustion strategy are very low relative to conventional diesel combustion. The minimum NO_x emission obtained is 0.03 g/h at a 60 °C intake air temperature.

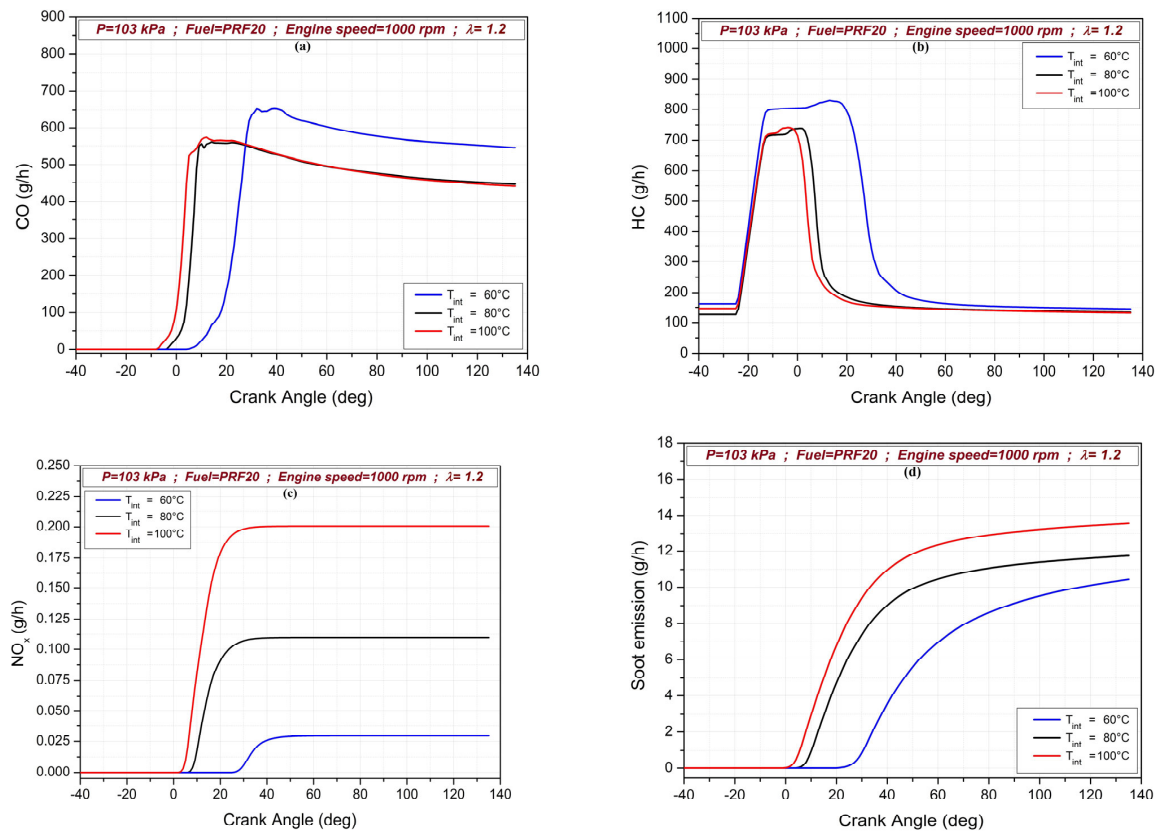


Figure 5. The effects of intake air temperature on (a) CO, (b) HC, (c) NO_x and (d) soot emissions.

3.2. Intake Manifold Pressure's Effects on RCCI Combustion

Figure 6 illustrates the change in the in-cylinder pressure and HRR at various intake manifold pressures and at a constant lambda value ($\lambda = 1.2$). The in-cylinder pressure rises as the intake manifold pressure increases. It is seen that the start of combustion advances when the intake manifold pressure increases. It is found that the combustion duration is dropped from 44 °CA to 38 °CA upon boosting the intake manifold pressure from 103 kPa to 140 kPa. It is observed that the maximum in-cylinder pressure is equal to 48 bar (at 7 °CA aTDC) at an intake manifold pressure of 140 kPa. In addition, the combustion is advanced with increased manifold pressure. The rise in auto-ignition reactions with increasing intake manifold pressure easily brings about combustion of the fuel. There are two stages of heat release—low temperature and high temperature—in RCCI combustion. The low-temperature reactions are advanced due to increased intake manifold pressure [46].

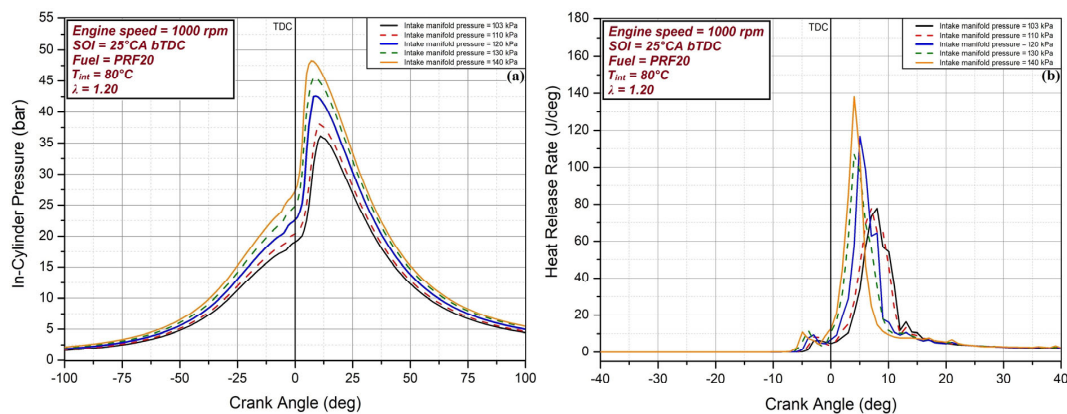


Figure 6. Change in (a) in-cylinder pressure and (b) HRR at various intake manifold pressures.

The effects of intake manifold pressure on HC, CO, NO_x and soot emissions for the RCCI combustion mode are seen in Figure 7. The nO_x and soot emission values increase due to the effect of rising in-cylinder temperature with increasing intake manifold pressure. The minimum value of NO_x emission is recorded as 0.110 g/h at a 103 kPa intake manifold pressure. In addition, an increase in HC and CO emissions is also observed as more charge is taken into the cylinder with the increase in intake manifold pressure. The maximum values of these emissions are obtained at 140 kPa intake manifold pressure. In the analyses performed in the closed cycle, it is observed that the HC emissions are at different values before direct injection with increasing intake manifold pressure, since approximately 8% of the residual exhaust gas formation was defined after combustion in the cylinder. As the intake manifold pressure increases, it can be stated that the emissions are released at lower crank angles with increasing temperature.

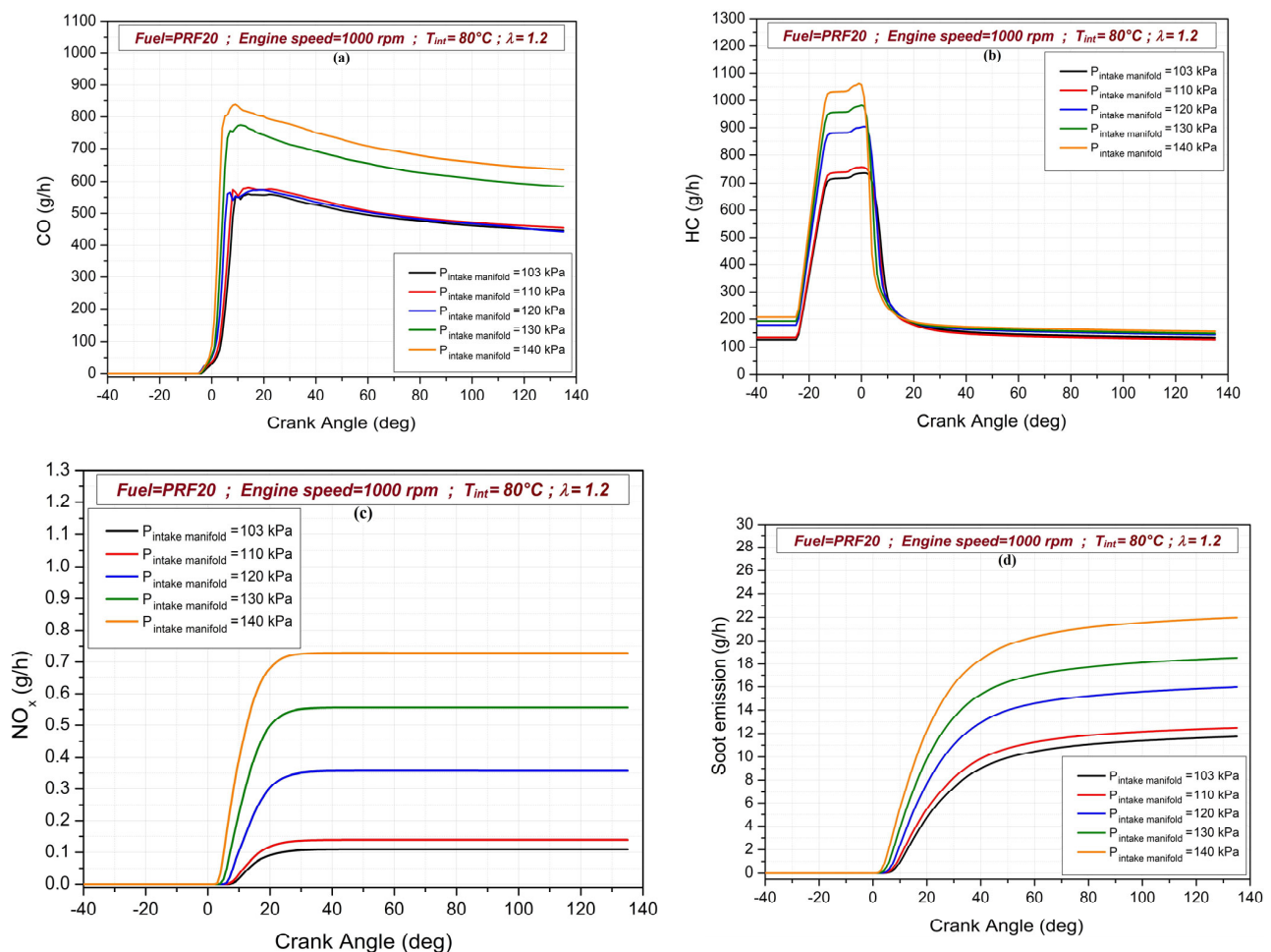


Figure 7. The effects of intake manifold pressure on (a) CO, (b) HC, (c) NO_x and (d) soot emissions.

3.3. Premixed Fuel Ratio's Effects on RCCI Combustion

The premixed fuel ratio's effects on RCCI combustion are demonstrated in Figure 8. The premixed fuel ratio significantly affects low-temperature combustion. The ignition timing delays, the cylinder pressure and the combustion rate decrease with a rise in the LRF in RCCI mode [59].

As can be seen, combustion is delayed with increasing premixed fuel ratio. This may be due to the decrease in fuel reactivity in the combustion chamber when the premixed LRF rises [60]. More HRF is injected directly a reduction in premixed fuel ratio. This causes the formation of richer regions in the combustion chamber before the combustion starts. It can be stated that combustion is controlled by n-heptane at low premixed fuel ratios [34].

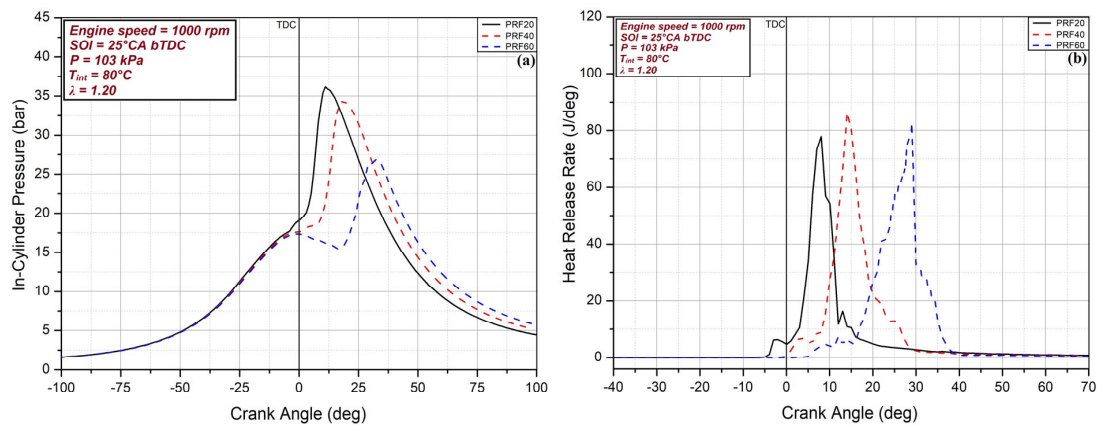


Figure 8. Change in (a) in-cylinder pressure and (b) HRR at various premixed ratios.

The maximum value of in-cylinder pressure was recorded as 36.15 bar (at 11 °CA aTDC) with the use of PRF20. When PRF20, PRF40 and PRF60 fuels are used, the combustion durations are obtained at 39 °CA, 18 °CA and 15 °CA, respectively.

The effects of premixed ratio variation on HC, CO, NO_x and soot emissions in RCCI combustion mode are shown in Figure 9. In general, it is seen that increasing the amount of iso-octane fuel in the mixture causes an increment in HC, CO and soot emissions. The minimum values of these emissions are recorded with PRF20 fuel. On the contrary, the NO_x emission values decrease. It can be concluded that this is caused by the reduction in the in-cylinder temperature with the increase in the percentage of iso-octane content in the mixture. The minimum NO_x emission obtained is 0.110 g/h with PRF60 fuel.

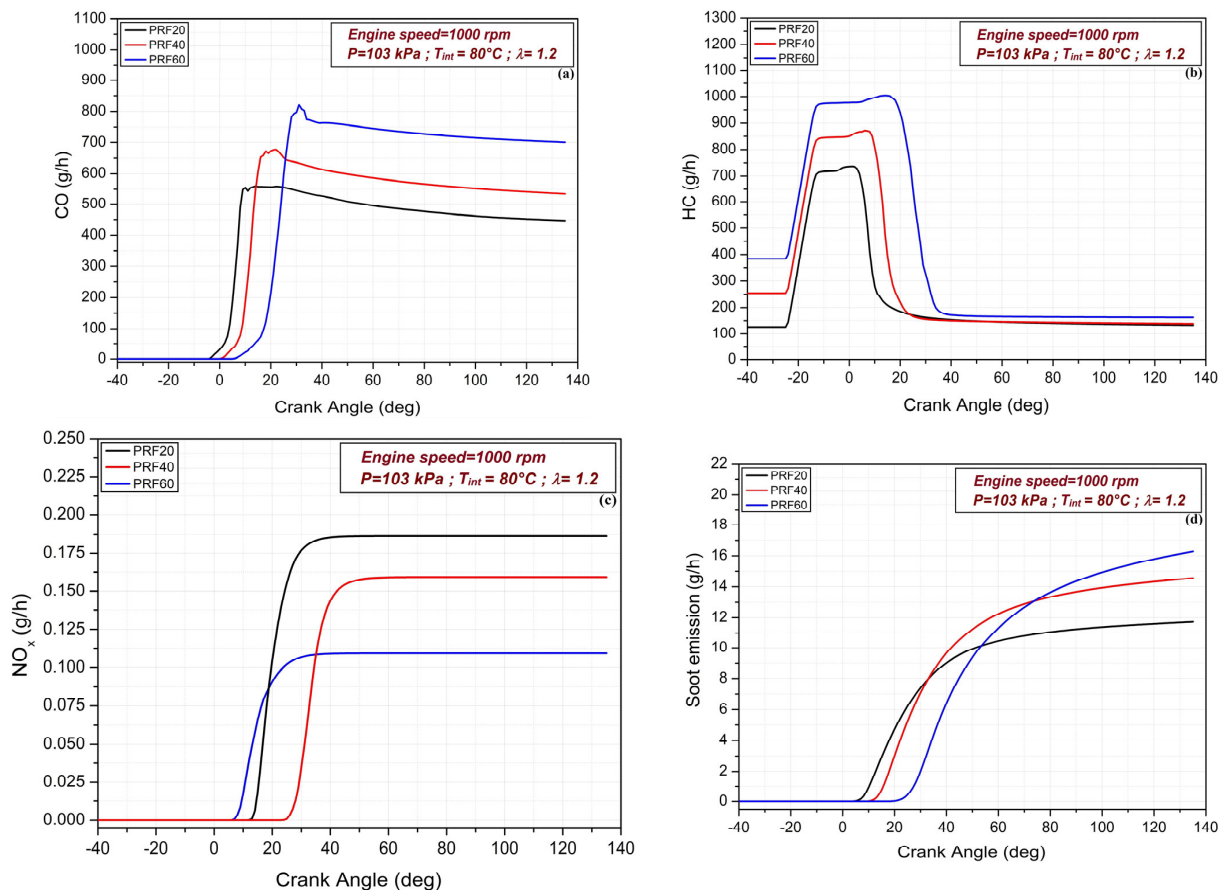


Figure 9. The effects of premixed ratio on (a) CO, (b) HC, (c) NO_x and (d) soot emissions.

It is not possible to experimentally obtain the distribution of equivalence ratio of the fuel and the in-cylinder temperature depending on the crank angle. These parameters were also analyzed numerically. The distribution of equivalence ratio for different premixed ratios is shown in Figure 10. The distribution of the fuels at different crank angles and the regions where they are concentrated were investigated depending on the PRF ratio change. The amount of iso-octane in the fuel mixture directly affects the equivalence ratio in the cylinder. Considering the equivalence ratio distribution, the formation of richer regions can be increased by reducing the amount of n-heptane in the mixture [61], which significantly affects the combustion efficiency.

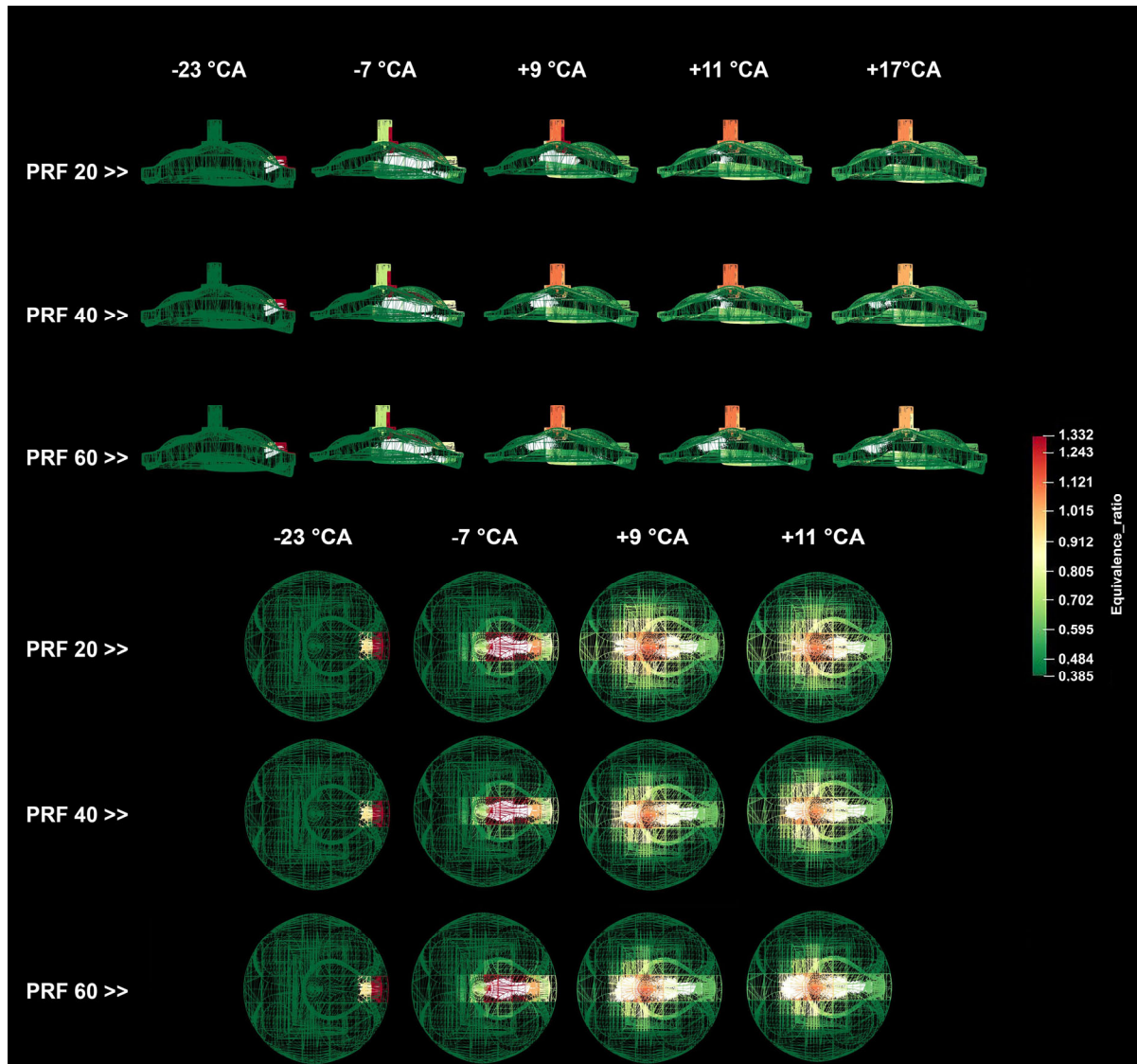


Figure 10. The distribution of equivalence ratio for different PRFs.

Figure 11 shows the distributions of in-cylinder mean temperature for the different premixed ratios. The numerical analysis results show that the maximum temperatures occur at 11 °CA, 31 °CA and 33 °CA aTDC for the fuels of PRF20, PRF40 and PRF60, respectively. As the PRF ratio increases, the amount of iso-octane in the mixture also increases, and thus, combustion is delayed due to the high octane number of iso-octane. Thereby, it is observed that the maximum temperatures in the cylinder for the three fuels occur at different crank angles.

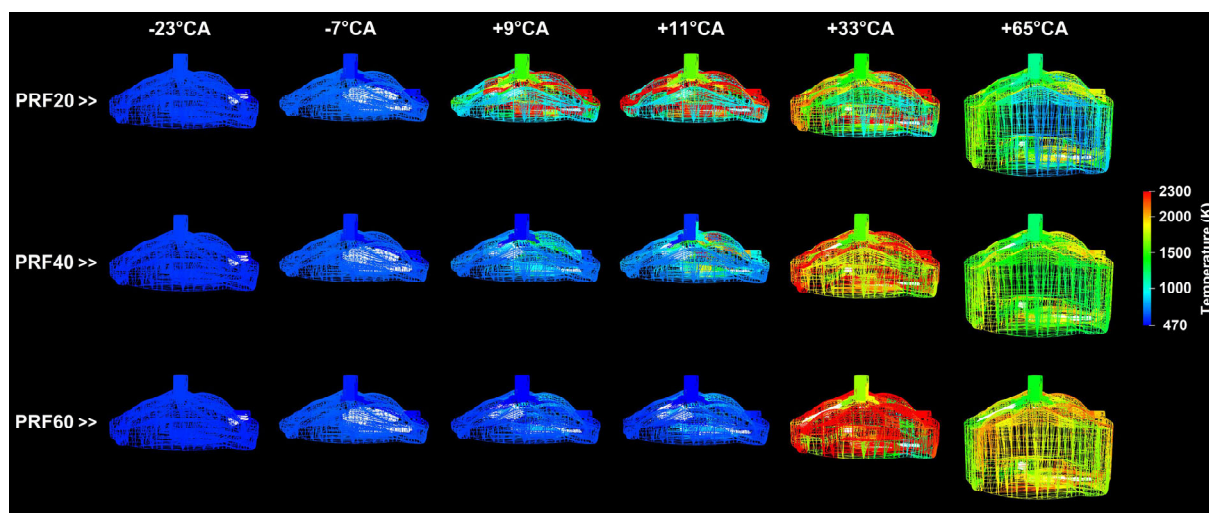


Figure 11. The distribution of in-cylinder mean temperature for different PRFs.

4. Conclusions

The aim of this study was to numerically research the effects of premixed ratio, intake manifold pressure and intake air temperature on RCCI combustion using n-heptane as an HRF and iso-octane as an LRF at a compression ratio of 9.2:1.

The in-cylinder pressure and HRRs for RCCI combustion were validated as being close to those under real conditions using the physical and chemical properties of the surrogate fuels (n-heptane and iso-octane) for diesel and gasoline. As a result of the analyses, it was found that intake air temperature, premixed fuel ratio and intake manifold pressure significantly affect RCCI combustion. There was a significant increase in reactivity in the combustion chamber with increasing intake air temperature. Therefore, the max. cylinder pressure also was increased, and combustion was advanced. The CA50 shifted by 18.5 °CA with an increment in the intake air temperature from 60 °C to 100 °C. As the intake charge mass increased, higher in-cylinder pressures were acquired by increasing the intake manifold pressure. In addition, combustion was advanced with increasing intake manifold pressure. It was observed that the combustion duration dropped from 44 °CA to 38 °CA upon boosting the intake manifold pressure from 103 kPa to 140 kPa. The combustion phasing was delayed as the premixed fuel ratio increased owing to the decrease in fuel reactivity in the combustion chamber. The maximum value of in-cylinder pressure was recorded as 36.15 bar (at 11 °CA aTDC) with the use of PRF20. This value was the highest in-cylinder pressure among all the in-cylinder pressure values obtained using all the fuels. It was shown that combustion delay occurred as the content of iso-octane in the fuel mixture was increased, and the maximum value of in-cylinder temperature obtained was 11 °CA aTDC using PRF20 fuel at the earliest point.

As the intake air temperature decreased, the in-cylinder temperature also dropped and incomplete combustion products were formed. Therefore, HC and CO emissions are much higher at low temperatures. The maximum values of these emissions were recorded at a 60 °C intake air temperature. However, the minimum NO_x emission obtained was 0.03 g/h at a 60 °C intake air temperature. As more charge was supplied to the cylinder with increasing intake manifold pressure, an increase in HC and CO emissions was also detected. The maximum values of these emissions were observed at a 140 kPa intake manifold pressure. The nO_x and soot emission values increased due to the effect of rising in-cylinder temperature with increasing intake manifold pressure. The minimum value of NO_x emission was recorded as 0.110 g/h at a 103 kPa intake manifold pressure. The maximum values of HC and CO emissions were recorded using PRF60 fuel since hydrocarbons were not fully combusted with an increase in the amount of iso-octane in the mixture. In addition, the minimum NO_x emission obtained was 0.110 g/h with PRF60 fuel

due to the decrease in the in-cylinder temperature with the rising proportion of iso-octane content in the mixture.

Considering the results of this study and similar studies, the operating range and combustion and emission characteristics of the alcohol-derived fuels that show good performance in RCCI combustion can be investigated experimentally or numerically in future studies. Also, optimization studies can be carried out using the response surface method for different fuel pairs. Moreover, the operating range can be extended using the variable compression ratio approach. Experimental and numerical studies can be carried out in this respect.

Author Contributions: S.H.: Conceptualization, Writing—Original Draft, Visualization, Software, Methodology, Validation. H.S.: Conceptualization, Funding Acquisition, Data Curation, Supervision. S.P.: Conceptualization, Methodology, Supervision. H.S.Y.: Conceptualization, Methodology, Supervision. All authors have read and agreed to the published version of the manuscript.

Funding: This research received no external funding.

Data Availability Statement: The data presented in this study are available on request from the corresponding author.

Acknowledgments: Hamit Solmaz and Serdar Halis were financially supported by the Scientific and Technological Research Council of Turkey (TÜBİTAK) to conduct this investigation. In addition, another source of financial funding from the United States National Science Foundation (Grant No: 1434273) was used in the experimental setup stage and for carrying out the experiments. The authors would like to thank TUBITAK, the United States National Science Foundation, Mahdi Shahbakhti (the previous director of the Energy Mechatronics Laboratory at Michigan Technological University) and Convergent Science Inc. for providing a free version of CONVERGE software.

Conflicts of Interest: The authors declare that there are no conflict of interest associated with this study.

Nomenclature

AMR	Adaptive Mesh Refinement
aTDC	After Top Dead Center
bTDC	Before Top Dead Center
CA	Crank Angle
CA50	Crank Angle Corresponding to 50% of the Total Heat Release
CFD	Computational Fluid Dynamics
CI	Compression Ignition
CO	Carbon Monoxides
COV _{IMEP}	Coefficient of Variation of IMEP
CR	Compression Ratio
DDM	Discrete Droplet Model
DI	Direct Injection
EGR	Exhaust Gas Recirculation
EVO	Exhaust Valve Opening
GDI	Gasoline Direct Injection
HC	Hydrocarbon
HCCI	Homogeneous Charged Compression Ignition
HRF	High-Reactivity Fuel
HRR	Heat Release Rate
IHRR	Integrated Heat Release Rate
IMEP	Indicated Mean Effective Pressure
ITE	Indicated Thermal Efficiency
IVC	Intake Valve Closing
KH	Kelvin–Helmholtz
LHV	Low Heat Value
LRF	Low-Reactivity Fuel

PFI	Port Fuel Injection
PRR	Pressure Rise Rate
NO _x	Nitrogen Oxides
PCCI	Premixed Charge Compression Ignition
PRF	Premixed Ratio Fuel
RANS	Reynolds Averaged Navier–Stokes
RCCI	Reactivity-Controlled Compression Ignition
RT	Rayleigh–Taylor
SFC	Specific Fuel Consumption
SI	Spark Ignition
SOC	Start of Combustion
SOI	Start of Injection
T _{IVC}	Intake Valve Closing Temperature
UHC	Unburned Hydrocarbons

References

- Reitz, R.D. Directions in internal combustion engine research. *Combust. Flame* **2013**, *1*, 1–8. [\[CrossRef\]](#)
- Verhaegh, J.; Kupper, F.; Willems, F. Data-Driven Air-Fuel Path Control Design for Robust RCCI Engine Operation. *Energies* **2022**, *15*, 2018. [\[CrossRef\]](#)
- Wang, Y.; Yao, M.; Li, T.; Zhang, W.; Zheng, Z. A parametric study for enabling reactivity controlled compression ignition (RCCI) operation in diesel engines at various engine loads. *Appl. Energy* **2016**, *175*, 389–402. [\[CrossRef\]](#)
- Iida, M.; Hayashi, M.; Foster, D.; Martin, J. Characteristics of homogeneous charge compression ignition (HCCI) engine operation for variations in compression ratio, speed and intake temperature while using n-butane as a fuel. *J. Eng. Gas Turbines Power* **2003**, *125*, 472–478. [\[CrossRef\]](#)
- Can, O.; Cinar, C.; Sahin, F. The investigation of the effects of premixed gasoline charge on HCCI-DI engine combustion and exhaust emissions. *J. Fac. Eng. Archit. Gazi Univ.* **2009**, *24*, 229–236.
- Hunicz, J.; Geca, M.S.; Kordos, P.; Komsta, H. An experimental study on a boosted gasoline HCCI engine under different direct fuel injection strategies. *Exp. Therm. Fluid Sci.* **2015**, *62*, 151–163. [\[CrossRef\]](#)
- Nagareddy, S. Temperature distribution measurement on combustion chamber surface of diesel engine-experimental method. *Int. J. Automot. Sci. Technol.* **2017**, *1*, 8–11.
- Krishnamoorthi, M.; Malayalamurthi, R.; He, Z.; Kandasamy, S. A review on low temperature combustion engines: Performance, combustion and emission characteristics. *Renew. Sustain. Energy Rev.* **2019**, *116*, 109404. [\[CrossRef\]](#)
- Uyumaz, A.; Aydoğan, B.; Calam, A.; Aksoy, F.; Yılmaz, E. The effects of diisopropyl ether on combustion, performance, emissions and operating range in a HCCI engine. *Fuel* **2020**, *265*, 116919. [\[CrossRef\]](#)
- Sharma, T.K.; Rao, G.A.P.; Madhumurthy, K. Combustion analysis of ethanol in HCCI engine. *Trends Mech. Eng. Technol.* **2012**, *3*, 1–9.
- Polovina, D.; McKenna, D.; Wheeler, J.; Sterniak, J.; Miersch-Wiemers, O.; Mond, A.; Hakan, Y. Steady-state combustion development of a downsized multi-cylinder engine with range extended HCCI/SACI capability. *SAE Int. J. Engines* **2013**, *6*, 504–519. [\[CrossRef\]](#)
- Ji, C.; Dec, J.E.; Dermotte, J.; Cannella, W. Effect of Ignition Improvers on the Combustion Performance of Regular-Grade E10 Gasoline in an HCCI Engine. *SAE Int. J. Engines* **2014**, *7*, 790–806. [\[CrossRef\]](#)
- Zhao, H. *HCCI and CAI Engines for the Automotive Industry*; Elsevier: Amsterdam, The Netherlands, 2007.
- He, B.Q.; Liu, M.B.; Zhao, H. Comparison of combustion characteristics of nbutanol/ethanol-gasoline blends in a HCCI engine. *Energy Convers. Manag.* **2015**, *95*, 101–109. [\[CrossRef\]](#)
- Nathan, S.S.; Mallikarjuna, J.; Ramesh, A. An experimental study of the biogas–diesel HCCI mode of engine operation. *Energy Convers. Manag.* **2010**, *51*, 1347. [\[CrossRef\]](#)
- Atkins, M.J.; Koch, C. The effect of fuel octane and diluent on homogeneous charge compression ignition combustion. *Proc. Inst. Mech. Eng. Part D J. Automob. Eng.* **2005**, *219*, 665–675. [\[CrossRef\]](#)
- Calam, A.; Icingur, Y. Effects of intake air temperature on combustion and performance of a HCCI engine. *J. Therm. Sci. Technol.* **2019**, *39*, 69–79.
- Bhaduri, S.; Jeanmart, H.; Contino, F. EGR control on operation of a tar tolerant HCCI engine with simulated syngas from biomass. *Appl. Energy* **2018**, *227*, 159–167. [\[CrossRef\]](#)
- Mofijur, M.; Hasan, M.M.; Mahlia, T.M.I.; Rahman, S.M.A.; Silitonga, A.S.; Ong, H.C. Performance and Emission Parameters of Homogeneous Charge Compression Ignition (HCCI) Engine: A Review. *Energies* **2019**, *12*, 3557. [\[CrossRef\]](#)
- Haraldsson, G.; Tunestål, P.; Johansson, B.; Hyvönen, J. *HCCI Combustion Phasing in a Multi Cylinder Engine Using Variable Compression Ratio*; SAE Technical Paper 2002-01-2858; SAE International: Warrendale, PA, USA, 2002.
- Peng, Z.; Zhao, H.; Ma, T.; Ladommatos, N. Characteristics of homogeneous charge compression ignition (HCCI) combustion and emissions of n-heptane. *Combust. Sci. Technol.* **2005**, *177*, 2113. [\[CrossRef\]](#)

22. Xu, F.; Wang, Z.; Yang, D.B.; Wang, J.X. Potential of high load extension for gasoline HCCI engine using boosting and exhaust gas recirculation. *Energy Fuels* **2009**, *23*, 2444–2452. [[CrossRef](#)]
23. Bai, G.; Ning, H. Investigation of intake boost pressure effects on performance and exhaust exergy of a natural gas fueled HCCI combustion engine. *Int. J. Eng. Innov. Res.* **2018**, *7*, 132–135.
24. Canakci, M. Combustion characteristics of a DI-HCCI gasoline engine running at different boost pressures. *Fuel* **2012**, *96*, 546–555. [[CrossRef](#)]
25. Khandal, S.V.; Banapurmath, N.R.; Gaitonde, V.N.; Hiremath, S.S. Paradigm shift from mechanical direct injection diesel engines to advanced injection strategies of diesel homogeneous charge compression ignition (HCCI) engines—A comprehensive review. *Renew. Sustain. Energy Rev.* **2017**, *70*, 369–384. [[CrossRef](#)]
26. Kokjohn, S.L.; Hanson, R.M.; Splitter, D.A.; Reitz, R.D. *Experiments and Modeling of Dual-Fuel HCCI and PCCI Combustion Using In-Cylinder Fuel Blending*; SAE Technical Paper 2009-01-2647; SAE International: Warrendale, PA, USA, 2009.
27. Reitz, R.D.; Hanson, R.M.; Splitter, D.A.; Kokjohn, S.L. Engine Combustion Control via Reactivity Stratification. U.S. Patent 8,616,177 B2, 31 December 2013.
28. Li, J.; Yang, W.; Zhou, D. Review on the management of RCCI engines. *Renew. Sustain. Energy Rev.* **2017**, *69*, 65–79. [[CrossRef](#)]
29. Harari, P.A.; Banapurmath, N.R.; Yaliwal, V.S.; Khan, T.M.Y.; Badruddin, I.A.; Kamangar, S.; Mahlia, T.M.I. Effect of injection timing and injection duration of manifold injected fuels in reactivity controlled compression ignition engine operated with renewable fuels. *Energies* **2021**, *14*, 4621. [[CrossRef](#)]
30. Hanson, R.M.; Kokjohn, S.L.; Splitter, D.A.; Reitz, R.D. An experimental investigation of fuel reactivity controlled PCCI combustion in a heavy-duty engine. *SAE Int. J. Engines* **2010**, *3*, 700–716. [[CrossRef](#)]
31. Wang, H.; Zhong, X.; Mi, S.; Yao, M. Numerical investigation on the combustion characteristics of PODE3/gasoline RCCI and high load extension. *Fuel* **2020**, *263*, 116366. [[CrossRef](#)]
32. Kokjohn, S.L. Reactivity Controlled Compression Ignition (RCCI) Combustion. Ph.D. Thesis, University of Wisconsin-Madison, Madison, WI, USA, 2012.
33. Eichmeier, J.; Reitz, R.D.; Rutland, C. A zero-dimensional phenomenological model for RCCI combustion using reaction kinetics. *SAE Int. J. Engines* **2014**, *7*, 106–119. [[CrossRef](#)]
34. Şahin, F.; Halis, S.; Yıldırım, E.; Altın, M.; Balaban, F.; Solmaz, H.; Yücesu, H.S. Effects of premixed ratio on engine operation range and emissions of a reactivity controlled compression ignition engine. *SAE Int. J. Fuels Lubr.* **2022**, *16*, 169–179. [[CrossRef](#)]
35. Uyumaz, A.; Solmaz, H. Experimental investigation of the effects of lambda and injection timing on combustion and performance characteristics in a RCCI Engine. *Gazi Univ. J. Sci. Part C Des. Technol.* **2016**, *4*, 299–308.
36. Ansari, E.; Poorghasemi, K.; Irdmousa, B.K.; Shahbakhti, M.; Naber, J. Efficiency and emissions mapping of a light duty diesel-natural gas engine operating in conventional diesel and RCCI modes. In Proceedings of the SAE 2016 International Powertrains, Fuels & Lubricants Meeting, Baltimore, MD, USA, 24–26 October 2016.
37. Kakaee, A.H.; Rahnama, P.; Paykani, A. Numerical study of reactivity controlled compression ignition (RCCI) combustion in a heavy-duty diesel engine using 3D-CFD coupled with chemical kinetics. *Int. J. Automot. Eng.* **2014**, *4*, 792–804.
38. Wu, Y.; Reitz, R.D. Effects of exhaust gas recirculation and boost pressure on reactivity controlled compression ignition engine at high load operating conditions. *J. Energy Resour. Technol.* **2015**, *137*, 032210. [[CrossRef](#)]
39. Liu, H.; Wang, X.; Zheng, Z.; Gu, J.; Wang, H.; Yao, M. Experimental and simulation investigation of the combustion characteristics and emissions using n-butanol biodiesel dual-fuel injection on a diesel engine. *Energy* **2014**, *74*, 741–752. [[CrossRef](#)]
40. Hasankola, S.S.M.; Shafaghhat, R.; Jahanian, O.; Amiri, S.T.; Shooghi, M. Numerical investigation of the effects of inlet valve closing temperature and exhaust gas recirculation on the performance and emissions of an RCCI engine. *J. Therm. Anal. Calorim.* **2020**, *139*, 2465–2474. [[CrossRef](#)]
41. Dziubak, T.; Karczewski, M. Experimental studies of the effect of air filter pressure drop on the composition and emission changes of a compression ignition internal combustion engine. *Energies* **2022**, *15*, 4815. [[CrossRef](#)]
42. Thomas, J.; West, B.; Huff, S. *Effect of Air Filter Condition on Diesel Vehicle Fuel Economy*; SAE International: Warrendale, PA, USA, 2013.
43. Dziubak, T.; Boruta, G. Experimental and theoretical research on pressure drop changes in a two-stage air filter used in tracked vehicle engine. *Separations* **2021**, *8*, 71. [[CrossRef](#)]
44. Dziubak, T.; Karczewski, M. Experimental study of the effect of air filter pressure drop on internal combustion engine performance. *Energies* **2022**, *15*, 3285. [[CrossRef](#)]
45. Arora, J.K. Design of Real-time Combustion Feedback System and Experimental Study of an RCCI Engine for Control. Ph.D. Thesis, Michigan Technological University, Houghton, MI, USA, 2016.
46. Polat, S.; Yucesu, H.S.; Uyumaz, A.; Kannan, K.; Shahbakhti, M. An experimental investigation on combustion and performance characteristics of supercharged HCCI operation in low compression ratio engine setting. *Appl. Therm. Eng.* **2020**, *180*, 115858. [[CrossRef](#)]
47. Heywood, J.B. *Internal Combustion Engine Fundamentals*; McGraw-Hill Education: New York, NY, USA, 2018.
48. Richards, K.; Senecal, P.; Pomraning, E. CONVERGE, version 2.2.0; Convergent Science Inc.: Madison, WI, USA, 2014.
49. Dukowicz, J.K. A particle-fluid numerical model for liquid sprays. *J. Comput. Phys.* **1980**, *35*, 229–253. [[CrossRef](#)]
50. Beale, J.C.; Reitz, R.D. Modeling spray atomization with the Kelvin-Helmholtz/ Rayleigh-Taylor hybrid model. *At. Sprays* **1999**, *9*, 623–650.

51. Convergent Science Inc. *CONVERGE (v2.3) Theory Manual*; Convergent Science Inc.: Madison, WI, USA, 2016.
52. Bahrami, S.; Poorghasemi, K.; Solmaz, H.; Calam, A.; Ipci, D. Effect of nitrogen and hydrogen addition on performance and emissions in reactivity controlled compression ignition. *Fuel* **2021**, *292*, 120330. [[CrossRef](#)]
53. Senecal, P.K.; Pomraning, E.; Richards, K.J.; Briggs, T.E.; Choi, C.Y.; McDavid, R.M.; Patterson, M.A. *Multi-Dimensional Modeling of Direct-Injection Diesel Spray Liquid Length and Flame Lift-Off Length Using CFD and Parallel Detailed Chemistry*; SAE Technical Paper 2003-01-1043; SAE International: Warrendale, PA, USA, 2003.
54. Luong, M.B.; Luo, Z.; Lu, T.F.; Chung, S.H.; Yoo, C.S. Direct numerical simulations of the ignition of lean primary reference fuel/air mixtures under HCCI condition. *Combust. Flame* **2013**, *160*, 2038–2047. [[CrossRef](#)]
55. Pohlkamp, K.; Reitz, R.D. *Reactivity Controlled Compression Ignition (RCCI) in a Single-Cylinder Air-Cooled HSDI Diesel Engine*; SAE International: Warrendale, PA, USA, 2012.
56. Hanson, R.; Reitz, R.D. *Transient RCCI Operation in a Light-Duty Multi-Cylinder Engine*; SAE International: Warrendale, PA, USA, 2013.
57. Kalghatgi, G.; Morganti, K.; Algunaibet, I.; Sarathy, M.; Dibble, R. *Knock Prediction Using a Simple Model for Ignition Delay*; SAE Technical Paper 2016-01-0702; SAE International: Warrendale, PA, USA, 2016.
58. Jia, M.; Dempsey, A.B.; Wang, H.; Li, Y.; Reitz, R.D. Numerical simulation of cyclic variability in reactivity-controlled compression ignition combustion with a focus on the initial temperature at intake valve closing. *Int. J. Engine Res.* **2014**, *16*, 441–460. [[CrossRef](#)]
59. Wang, H.; Zheng, Z.; Liu, H.; Yao, M. Combustion mode design with high efficiency and low emissions controlled by mixtures stratification and fuel reactivity. *Front. Mech. Eng.* **2015**, *1*, 8. [[CrossRef](#)]
60. Zou, X.; Wang, H.; Zheng, Z.; Reitz, R.D.; Yao, M. *Numerical Study of the RCCI Combustion Processes Fuelled with Methanol, Ethanol, n-Butanol and Diesel*; SAE Technical Paper 2016-01-0777; SAE International: Warrendale, PA, USA, 2016.
61. Mohammadian, A.; Chehrmonavari, H.; Kakaee, A.; Paykani, A. Effect of injection strategies on a single-fuel RCCI combustion fueled with isobutanol/isobutanol+DTBP blends. *Fuel* **2020**, *278*, 118219. [[CrossRef](#)]

Disclaimer/Publisher's Note: The statements, opinions and data contained in all publications are solely those of the individual author(s) and contributor(s) and not of MDPI and/or the editor(s). MDPI and/or the editor(s) disclaim responsibility for any injury to people or property resulting from any ideas, methods, instructions or products referred to in the content.